Non-linear finite element analysis of an elastic structure loaded by hydrostatic following forces

Christophe Hoareau, Jean-François Deü

Available online at www.sciencedirect.com

ScienceDirect

Procedia Engineering 199 (2017) 1302–1307

Procedia Engineering

www.elsevier.com/locate/procedia

X International Conference on Structural Dynamics, EURODYN 2017

Non-linear finite element analysis of an elastic structure loaded by hydrostatic follower forces

C. Hoareau[a], J.-F. Deü[a]

[a]*LMSSC, Conservatoire National des Arts et Métiers, 292 Rue Saint-Martin, Paris 75003, France*

Abstract

This study deals with the non-linear finite element computation of thin flexible structures loaded by hydrostatic forces due to the presence of an internal liquid at rest. In aerospace application, the dynamic behaviour of structures containing an inviscid incompressible fluid (i.e. launcher with liquid propellant, tank of satellite, etc.) is generally computed considering an equilibrium state resulting from a linear fluid-structure interaction problem. It is important to note that in this case, the gravity plays an important role in vibrations and the so called elastogravity operator should be taken into account [1,2]. In the present work, we consider the large deformation behavior of a structure loaded by hydrostatic follower forces in order to obtain an accurate static equilibrium state. The solution is computed using a Newton-Raphson algorithm considering the geometrical and material tangent stiffness matrices as well as the contribution of the follower forces [3]. Those linearized operators of the iterative algorithm are used to compute the dependancy between the incremental horizontal level of the free surface, under the fluid volume conservation constraint [4]. Special attention is paid to the finite element discretization of the wetted surface, considering a level-set method [6,7]. Some numerical examples are analyzed to show the efficiency of the proposed approach.

Peer-review under responsibility of the organizing committee of EURODYN 2017.

Keywords: Large deformation; Hydrostatic fluid loading; Finite element method ;

1. Introduction

Computation of the dynamic behavior of a flexible tank containing a heavy fluid is often studied in aerospace engineering (i.e. launcher with liquid propellant, tank of satellite, etc.). Before performing any dynamic analysis of the coupled fluid-structure system, a quasi-static equilibrium state can be obtained using a linearization around the reference configuration. This linearization leads to a non-conventional elastogravity operator [1,2]. In the present paper we propose a finite-element approach able to compute the structural pre-stressed state considering material and geometrical nonlinearities. The objective is to take into account the effect of the fluid (assumed at rest and incompressible) on the structure, without volumetric mesh of the fluid domain. The idea is to compute hydrostatic follower forces acting on the wetted surface of the structure. Expected results are the quasi-static equilibrium states

* Corresponding author. Tel.: +0-000-000-0000 ; fax: +0-000-000-0000.
E-mail address: christophe.hoareau@lecnam.net

1877-7058
Peer-review under responsibility of the organizing committee of EURODYN 2017.
10.1016/j.proeng.2017.09.320

from an empty to a fulfilled state of the tank. A technical difficulty of the numerical method is due to the inviscid fluid hypothesis: the wetted surface does not remain coincident with the initial mesh at the fluid-structure interface. One of the main contributions of this article lies on the use of a flexible level-set method which takes into account the discontinuity of the wetted surface. The outline of the paper is the following. In section 2 we present the fluid-structure hypotheses. Section 3 deals with the finite element formulation in the reference configuration. In section 4, we detail the linearization of the virtual external work used in the Newton-Raphson algorithm. This leads to the construction of the follower forces tangent stiffness matrix defined in a curved elementary surface. In section 5, the level-set method [6,7] is introduced to overcome the slip condition difficulty at the fluid-structure interface. Note that we also satisfy the fluid volume conservation. In section 6, a numerical example from [4] is studied to evaluate the convergence rate of our method and compare our results with the literature.

2. Reference problem

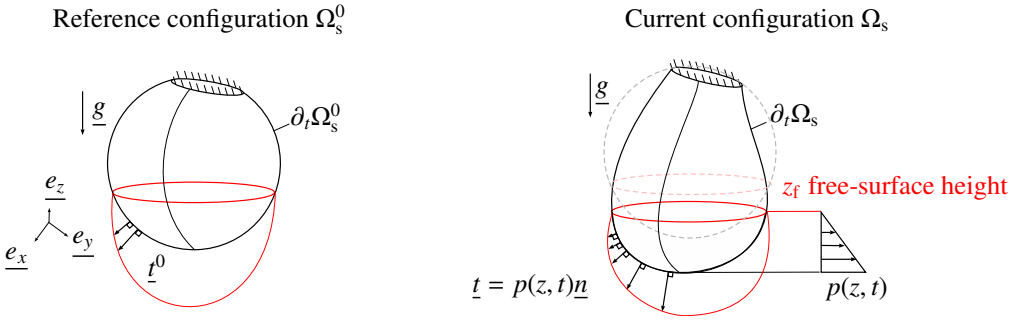

Fig. 1. Structure in its reference configuration and its current configuration loaded by a hydrostatic following forces (only the internal face of the tank with the follower forces are represented)

Let's assume a hyperelastic model for the structure and an invicid incompressible model for the heavy fluid. The fluid loading corresponds to a hydrostatic pressure $p(z,t)$ supported by the normal $\underline{n}$ at the current fluid-structure interface, also called the wetted surface. The hydrostatic pressure field is define in $\partial_t\Omega_s$ as

$$\begin{aligned} p(\underline{x},t) &= 0 \qquad\qquad \text{if} \quad z \geqslant z_f(t) \\ p(\underline{x},t) &= -\rho_f g(z - z_f) \qquad \text{if} \quad z < z_f(t) \end{aligned} \tag{1}$$

where ρ_f is the fluid density and z_f the free-surface height. An additional constrain has to be taken into account : the internal fluid volume contained below the free-surface eight is contant.

3. Finite element formulation of the non-linear problem

The variational formulation of the NL structural problem in its current configuration is classicaly [5] written as

$$-\int_{\Omega_S} \underline{\underline{\sigma}} : \underline{\underline{\delta d}}\, dv + \int_{\partial_t\Omega_S} \underline{t} \cdot \underline{\delta u}\, ds = 0, \quad \forall\, \underline{\delta u} \in C_u \tag{2}$$

where $\underline{\underline{\sigma}}$ is the Cauchy strain tensor, $\underline{\underline{\delta d}}$ is the rate of deformation tensor and C_u the admissible space of displacement functions assumed smooth enought. This formualtion is written in the reference configuration as

$$-\int_{\Omega_s^0} \mathbb{S} : \delta\dot{\mathbb{E}}\, dV + \int_{\partial_t\Omega_s^0} \underline{t_0} \cdot \underline{\delta u}\, dS = 0, \quad \forall\, \underline{\delta u} \in C_u \tag{3}$$

where $\mathbb{S}$ and $\mathbb{E}$ are respectively the second Piola-Kirchhoff stress tensor and the Green-lagrange strain tensor. Under the assumption of large displacements and small strains, we consider a Saint-Venant Kirchhoff constitutive law

$\mathbb{S} = 2\mu\mathbb{E} + \lambda tr(\mathbb{E})\,\mathbb{I}$. The finite element discretization of the variational formulation leads to the non-linear equation written as

$$\underline{F_{\text{int}}}(\underline{q}) - \underline{F_{\text{ext}}}(\underline{q}) = \underline{0} \tag{4}$$

where $\underline{F_{\text{int}}}$ and $\underline{F_{\text{ext}}}$ are respectively the internal and external force vectors and $\underline{q}$ the unknown nodal displacement vector. An iterative algorithm based on a Newton-Raphson method leads to the resolution of linearized equations defined by

$$\mathbb{K}_{\text{tan}}\underline{\Delta q} = \underline{R} \tag{5}$$

where $\underline{R}$ is the residual vector and $\mathbb{K}_{\text{tan}}$ the tangent stiffness matrix. This operator is the summation of the material tangent matrix $\mathbb{K}_{\text{mat}}$, the geometric tangent matrix $\mathbb{K}_{\text{geo}}$ and the follower forces contribution $\mathbb{K}_{\text{pres}}$. This last tangent stiffness matrix is detailled in the following section.

4. Follower forces contribution

The external virtual work which depends on the free-surface height z_{f} and the current position of the wetted-surface, is written as

$$\delta W_{\text{pres}} = -\int_{\partial_t\Omega_{\text{s}}} \underline{\delta u}\cdot p(z,t)\underline{n}ds \quad \text{with} \quad p(z,t) = -\rho_{\text{f}}\, g\,(z - z_{\text{f}}) \tag{6}$$

The discretized virtual external work leads to the construction of the external nodal force vector $\underline{F_{\text{ext}}}$ such that

$$\delta W^h_{\text{pres}} = \underline{\delta q}^T\, \underline{F_{\text{ext}}}(\underline{q}) \tag{7}$$

and its linearization gives the expression of the tangent stiffness $\mathbb{K}_{\text{pres}}$ such that

$$\Delta\delta W^h_{\text{pres}} = \underline{\delta q}^T \mathbb{K}_{\text{pres}}\, \underline{\Delta q} \tag{8}$$

in which $\underline{\delta q}$ is the virtual nodal displacement.

4.1. Linearized virtual external work

In order to evaluate $\mathbb{K}_{\text{pres}}$, we use a truncated Taylor expansion of the virtual external work given by

$$\Delta\delta W_{\text{pres}} = -\int_{\partial_t\Omega_{\text{s}}} \underline{\delta u}\cdot\left(\Delta p(z,t)\underline{n} + p(z,t)\underline{\Delta n}\right)ds = \Delta\delta W^p_{\text{pres}} + \Delta\delta W^n_{\text{pres}} \tag{9}$$

where $\Delta\delta W^p_{\text{pres}}$ and $\Delta W^n_{\text{press}}$ are respectively the contribution of the pressure field variation and the external normal variation. We can develop $\Delta\delta W^p_{\text{pres}}$ as a function of the structural displacement and the vertical free-surface displacement as

$$\Delta\delta W^p_{\text{pres}} = -\int_{\partial_t\Omega_{\text{s}}} \underline{\delta u}\cdot\left(-\rho_{\text{f}}\, g\,\left(\Delta u_z - \Delta u_{z_{\text{f}}}\right)\right)\underline{n}ds \quad \text{because} \quad \Delta z - \Delta z_{\text{f}} = \Delta u_z - \Delta u_{z_{\text{f}}} \tag{10}$$

and $\Delta u_{z_{\text{f}}}$ is related to $\underline{\Delta u}$ by the following relation

$$\Delta u_{z_{\text{f}}} = \frac{\Delta V}{A_{\text{f}}} = \frac{\displaystyle\int_{\partial_t\Omega_{\text{s}}} \underline{\Delta u}\cdot\underline{n}ds}{\displaystyle\int_{\partial_t\Omega_{\text{s}}} \underline{n}\cdot\underline{e_z}ds} \tag{11}$$

where A_{f} is the free-surface area and ΔV is the volume change due to the wetted surface normal displacement as illustrated in Fig. 2.
Thus, $\Delta\delta W^p_{\text{pres}}$ is given by

$$\Delta\delta W^p_{\text{pres}} = \rho_{\text{f}}\, g\int_{\partial_t\Omega_{\text{s}}} \underline{\delta u}\cdot\left(\underline{\Delta u}\cdot\underline{e_z} - \frac{1}{A_{\text{f}}}\int_{\partial_t\Omega_{\text{s}}} \underline{\Delta u}\cdot\underline{n}ds\right)\underline{n}ds \tag{12}$$

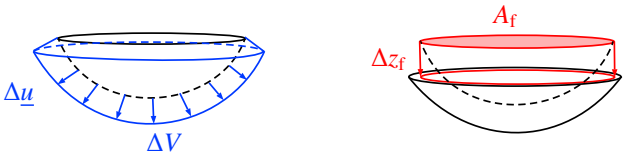

Fig. 2. Geometric relation between the volume variation and the free-surface height

4.2. Discretized tangent stiffness matrix

In practice, it is usefull to express the discretized elementary matrices defined in an elementary surface. Using the nodal current position $\underline{x}^{\mathrm{e}}$ and the shape function matrix $\underline{\underline{\Phi}}^{\mathrm{e}}$, the evaluation of the tangent stiffness matrices of the follower forces (Eq. 9) leads to a variable change detailled below

$$\int_{\partial_t \Omega_s^{\mathrm{e}}} \underline{n} ds = \int_{-1}^{1}\int_{-1}^{1} \left(\frac{\partial \underline{x}^{\mathrm{e}}}{\partial \xi} \wedge \frac{\partial \underline{x}^{\mathrm{e}}}{\partial \eta} \right) d\xi d\eta = \int_{-1}^{1}\int_{-1}^{1} \underline{n}^{\mathrm{e}} d\xi d\eta \tag{13}$$

where $\underline{n}^{\mathrm{e}}$ is the non-unitary external normal of a surfacic element. The external unit normal variation is given by

$$\int_{\partial_t \Omega_s^{\mathrm{e}}} \underline{\Delta n} ds = \int_{-1}^{1}\int_{-1}^{1} \left(\frac{\partial \underline{x}^{\mathrm{e}}}{\partial \xi} \wedge \frac{\partial \underline{\Delta x}^{\mathrm{e}}}{\partial \eta} - \frac{\partial \underline{x}^{\mathrm{e}}}{\partial \eta} \wedge \frac{\partial \underline{\Delta x}^{\mathrm{e}}}{\partial \xi} \right) d\xi d\eta = \int_{-1}^{1}\int_{-1}^{1} \left(\frac{\partial \underline{x}^{\mathrm{e}}}{\partial \xi} \wedge \frac{\partial \underline{\underline{\Phi}}^{\mathrm{e}}}{\partial \eta} - \frac{\partial \underline{x}^{\mathrm{e}}}{\partial \eta} \wedge \frac{\partial \underline{\underline{\Phi}}^{\mathrm{e}}}{\partial \xi} \right) d\xi d\eta \underline{\Delta q^{\mathrm{e}}} \tag{14}$$

The previous equations give us an expression between the external unit normal of the wetted surface and the position vector in the current configuration. The development of $\Delta\delta W^{pe}_{\mathrm{pres}}$ and $\Delta\delta W^{ne}_{\mathrm{pres}}$ in an elementary surface are given by

$$\Delta\delta W^{pe}_{\mathrm{pres}} = \underline{\delta q^{\mathrm{e}T}} \left\{ \rho_f g \int_{-1}^{1}\int_{-1}^{1} \underline{\underline{\Phi}}^{\mathrm{e}T} \underline{n}^{\mathrm{e}} \underline{e}_z^T \underline{\underline{\Phi}}^{\mathrm{e}} d\xi d\eta - \frac{\rho_f g}{A_{\mathrm{fs}}} \left(\int_{-1}^{1}\int_{-1}^{1} \underline{\underline{\Phi}}^{\mathrm{e}T} \underline{n}^{\mathrm{e}} d\xi d\eta \right) \left(\int_{-1}^{1}\int_{-1}^{1} \underline{n}^{\mathrm{e}T} \underline{\underline{\Phi}}^{e} d\xi d\eta \right) \right\} \underline{\Delta q^{\mathrm{e}}} \tag{15}$$

and

$$\Delta\delta W^{ne}_{\mathrm{pres}} = \underline{\delta q^{\mathrm{e}T}} \left\{ - \int_{-1}^{1}\int_{-1}^{1} \underline{\underline{\Phi}}^{\mathrm{e}T} p(z,t) \left(\frac{\partial \underline{x}^{\mathrm{e}}}{\partial \xi} \wedge \frac{\partial \underline{\underline{\Phi}}^{\mathrm{e}}}{\partial \eta} - \frac{\partial \underline{x}^{\mathrm{e}}}{\partial \eta} \wedge \frac{\partial \underline{\underline{\Phi}}^{\mathrm{e}}}{\partial \xi} \right) d\xi d\eta \right\} \underline{\Delta q^{\mathrm{e}}} \tag{16}$$

From those two equations, we obtain $\mathbb{K}^{pe}_{\mathrm{press}}$ (see Eq. 15) and $\mathbb{K}^{ne}_{\mathrm{press}}$ (see Eq. 16) which depend on the wetted-surface and the unknown nodal displacement vector. An assembly operation in all finite elements leads to the global tangent stiffness matrix.

5. Wetted surface discretization

5.1. Slip condition at the fluid-structure interface

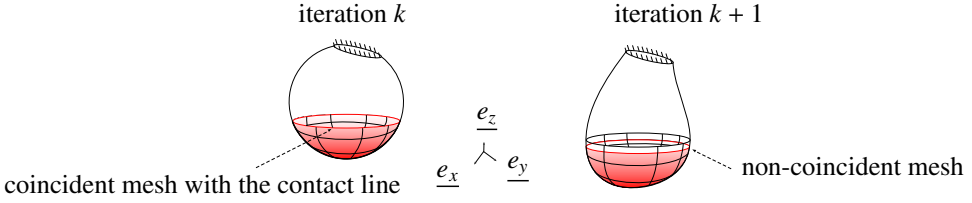

Fig. 3. Change of the wetted surface at each Newton-Raphson iterations

The fluid is supposed inviscid, thus a slip condition at the wetted surface leads to a transformation of surface boundary (the contact line). Consequently, the initial discretization of the wetted surface is no more appropriate at each iteration step. This problem has to be taken into account in the simulation as shown in Fig. 3 and numerous solutions as level-set method (illustrated in Fig. 4) or remeshing can be done to overcome the difficulty.

5.2. Level set method

The pressure field can be taken into account with a level-set method [6,7]. Numerical intregration based on a Gaussian quadrature can be done with no dependance with the initial mesh. An important step of element spliting is performed to find the position of Gauss points, as shown in Fig. 5.(a). Significant efforts have been made to make the splitting-step algorithm as flexible as possible according to the 3D meshing. Thus, any surface discretized with quadrilaterals elements with height nodes can be easily used in our code without extra manipulations for the user.

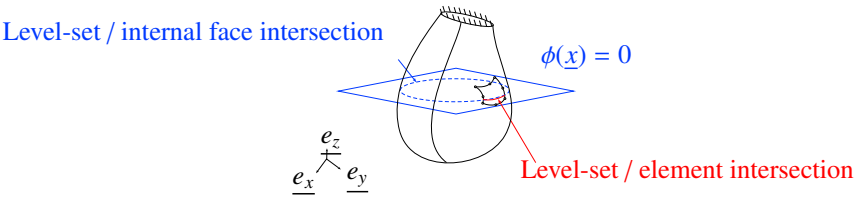

Fig. 4. Level-set intersections with the internal face and Level-set intersetcion with a surfacic element

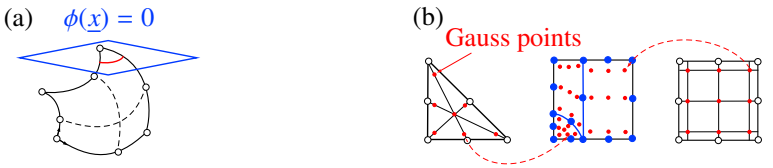

Fig. 5. (a) Cutted element by the level-set in the real configuration ; (b) Splitting of the element with Gauss points in the reference configuration

5.3. Fluid volume conservation

In this section, we detail a method based on Gauss's theorem wich allow the calculation of the fluid volume without any volumetric mesh. Let's consider Ω_f a domain bounded by the wetted surface S_w and the free surface S_f. For a piecewise vector field $(z - z_\mathrm{f})\underline{e_z}$, such that $\mathrm{div}\left((z - z_\mathrm{f})\underline{e_z}\right) = 1$, the internal volume calculation is written as

$$V_\mathrm{f} = \int_{\Omega_\mathrm{f}} dV = \int_{\Omega_\mathrm{f}} \mathrm{div}\left((z - z_\mathrm{f})\underline{e_z}\right) dV = \int_{S_\mathrm{w}} (z - z_\mathrm{f})\underline{e_z} \cdot \underline{n} ds \tag{17}$$

where the term on the free-surface vanish because the surface is assumed to be horizontal. The fluid volume calculation can be used in our algorithm to satisfy the incompressibility constrain, without volumetric mesh of the fluid domain.

6. Numerical examples: elastic hollow hook

A 3D finite-element code with a level-set method has been developed to solve non-linear hydrostatic problem. To validate our approach, an example illustred in Fig. 6 from the literature [4] is analyzed. This example concerns the computation of the finite deformation of an elastic hollow hook filled with liquid. The geometry is described in Fig. 6 (a) and the simplest hyperelastic material model (i.e. the Saint-Venant Kirchhoff model) is used as constitutive relation for the structure. The Young modulus and the Poisson ratio are respectively $E = 1$ GPa and $\nu = 0.3$. Two types of simulations have been set up. The first one is a filling simulation step by step that allow us to obtain each quasi-static equilibrium position from the empty state to a filled state. As an example of results, a deformed geometry at a chosen step of the simulation is plotted in Fig. 6 (b). Fig. 7 (a) shows the evolution of the displacement of the point A and the free-surface area in terms of the free-surface height. The second simulation is a one-step simulation, from the empty state to a filled state. In Fig. 8 (b) we plot the L_2 norm of the out-of-balance residual vector. It can be observed that the slope of the convergence rate of our algorithm is almost linear validating the robustness of our Newton-Raphson algorithm.

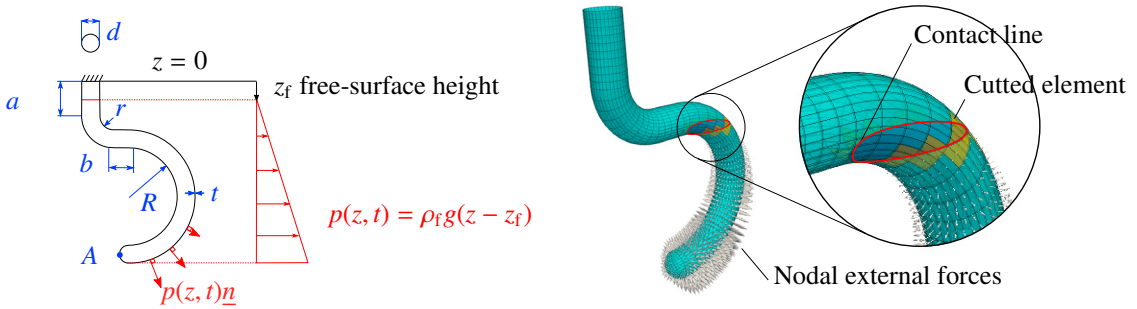

Fig. 6. (a) Elastic hollow hook from [4] with d = 10 cm, a = 20 cm, r = 10 cm, R = 25 cm, t = 0.2 cm, ρ_f = 1000 kg.m^{-3} and g = 9.81 m.s^{-}2 ; (b) Cutted elements by the level-set and visualization of the follower forces on the FE mesh.

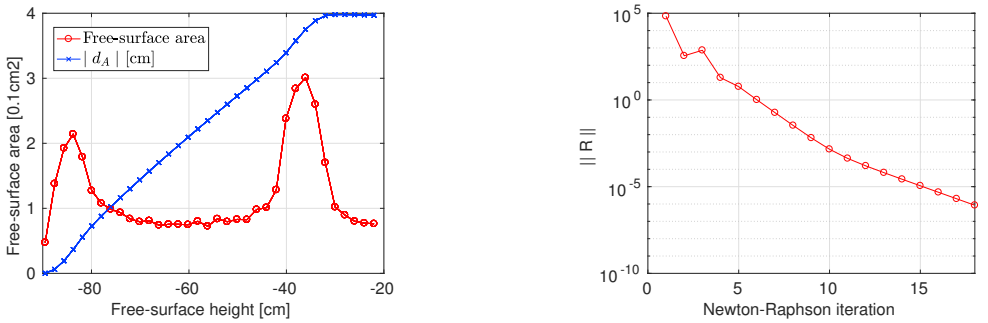

Fig. 7. (a) Displacement of point A | d_A | and free-surface area A_{fs} vs free-surface height from a simulation step by step; (b) Convergence rate of the L_2 norm of the out-of-balance residual vector of a one-step simulation from V_f = 0 m^3 to V_f = 9.8.10^{-3} m^3

Comparisons between our results and those from [3] show a slight difference in the converged maximum displacement of point A. Even with a fine mesh (around 780 000 dofs) we obtain a solution of 4.02 cm instead of 4.36 cm according to [3]. This may be due to our 3D hexahedric finite element model instead of their shell model, which may lead to different boundary conditions.

7. Conclusion and outlooks

Two specifics points are highlighted in this paper. At first, a non-linear finite-element formulation taking into account the hydrostatic follower forces and the fluid volume conservation constrain, is detailed. The associated resolution method necessitates the derivation of non-standard tangent stiffness operators. Secondly, an accurate resolution method, based on a level-set approach, is developed to solve the problem. Finally, an application to an elastic hollow hook filled with liquid is proposed. Despite some differences between our model and results from the literature, the computation of the quasi-static geometrical non-linear solution shows a satisfactory rate of convergence of our iterative resolution method. Furthermore, the obtained results can directly be used for a dynamic analysis around the pre-stressed equilibrium state.

References

[1] H.J.P. Morand, R. Ohayon, Fluid-Structure Interaction, Wiley, 1995.
[2] J.S. Schotté, R. Ohayon, Linearized formulation for fluid-structure interaction: Application to the linear dynamic response of a pressurized elastic structure containing a fluid with a free surface, J. Sound Vibration 332 (2013) 2396–2414.
[3] H.D. Hibbitt, Some Follower Forces and Load Stiffness, Int. J. Numer. Methods Engrg. 14 (1979) 937–941.
[4] T. Rumpel, K. Schweizerhof, Hydrostatic fluid loading in non-linear finite element analysis, Int. J. Numer. Methods Engrg. 59 (2004) 849–870.
[5] O.C. Zienkiewicz, R.L. Taylor, The Finite Element Method: Solid mechanics, Butterworth-Heinemann, 2000.
[6] J.A. Sethian, A fast marching level set method for monotonically advancing fronts, Proc. Natl. Acad. Sci. U.S.A. 93 (1996) 1591–1595.
[7] N. Moës, T. Belytschko, A finite element method for crack growth without remeshing, Int. J. Numer. Methods Engrg. 46 (1999) 131–150.